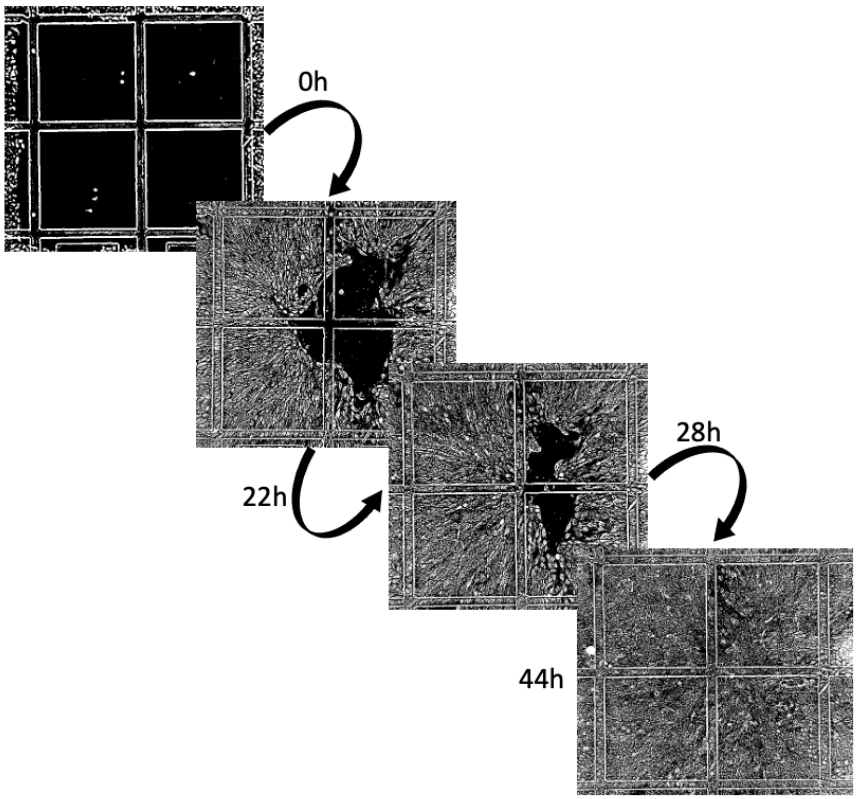

Using open-volume microfluidics to develop gap closure assay in a confluent monolayer of cells

Master's thesis at Fluicell AB

DAVID PERHED

DEPARTMENT OF LIFE SCIENCES
CHALMERS UNIVERSITY OF TECHNOLOGY
Gothenburg, Sweden 2023
www.chalmers.se

Master's thesis 2023

Using open-volume microfluidics to develop gap closure assay in a confluent monolayer of cells

DAVID PERHED

CHALMERS
UNIVERSITY OF TECHNOLOGY

Department of Life Sciences
Chalmers University of Technology
Gothenburg, Sweden 2023

David Perhed

Supervisor: Tatsiana Lobovkina, Fluicell AB
Co-supervisor: Adina Lupu, Fluicell AB
Examiner: Annikka Polster, Systems and Synthetic Biology

Master's Thesis 2023
Department of Life Sciences
Chalmers University of Technology
SE-412 96 Gothenburg
Telephone +46 31 772 1000

Typeset in LaTeX
Printed by Chalmers Reproservice
Gothenburg, Sweden 2023

Abstract

Understanding the basic mechanisms of wound healing in living organisms is important to enhance healing as well as to avoid infections and scarring. Today, cell-free areas (gaps) in a confluent monolayer of cells *in vitro*, are commonly formed to mimic wounds *in vivo*. Migration and proliferation of cells are essential mechanisms for gap closure, *in vitro*. In many studies, measuring cell migration is of interest, thus suppressing cell proliferation is desired. Standard gap closure assays provide simple ways of monitoring cell migration *in vitro*. Commonly, these assays focus on formation of gaps with simple geometries, such as lines circles, squares and triangles. Other methods for gap formation have therefore been developed, however these methods have limited flexibility of forming gaps with arbitrary size and geometry. This study aims to use open-volume microfluidics to develop an *in vitro* gap-closure assay, allowing for time-dependent gap closure to be monitored and analysed for gaps with different initial geometry. Gaps of different initial geometries and sizes were successfully formed in a confluent monolayer of HaCaT cells. Gap closure of square, circle and crescent moon geometries (300x300 μm) was monitored under conditions where cells were allowed to proliferate and under conditions of no proliferation. Additionally, gap closure of larger square gaps (1000x1000 μm) was monitored under conditions of proliferation. This study developed an assay serving as a foundation for future studies of HaCaT gap closure *in vitro*. Furthermore, the study provides insights about printing fibronectin with the Biopixlar technology, important for modulating cellular migration and adhesion during gap closure. These conclusions, further add to the current research field of gap closure assays and provides principal knowledge needed for future studies aiming towards formation of gaps with more complex geometries.

Acknowledgements

I would like to express appreciation towards everyone that has supported me with this study. I cannot begin to express my thanks to Dr Tatsiana Lobovkina, my research supervisor, for her support in both writing and guiding the project. In addition, this thesis would not have been possible without the support and nurturing of Adina Lupu, my co-supervisor. Thank you for teaching me about all the techniques used in this project and for all support in gathering experimental results. Working together with you was a pleasant experience! I would also like to extend my sincere thanks to Dr Vladimir Kirejev, for wisdom about the printing technology. Thank you for always answering questions and supporting with experiments if needed. Furthermore, I'd like to recognize the assistance that I received from Anton Rydberg. Many thanks for your practical suggestions about cell culturing and helpful advice of the printing process. Moreover, I gratefully acknowledge the help from Dr Andreas Svanström and Dr Sanna Sämfors. Thank you supporting me with the printing software and always answering questions. Finally, I would like to extend my special thanks everyone at Fluicell for welcoming me during my thesis project. Thank you for all laughs and all moments of learning you have provided me with.

Contents

1
Introduction

Wound healing is a complex cellular and biochemical process, essential for tissue repair in living organisms [1]. Therefore, understanding the mechanisms of wound closure is necessary to avoid outcomes such as scarring and infections [2]. To imitate this process *in vitro*, cell-free areas, referred to as gaps, are commonly formed in a confluent layer of cells [3]. Consequently, assays of gap closure are an attractive tool allowing for *in vitro* studies before starting *in vivo* experiments [4]. Today, one of the most common techniques for obtaining gaps in a confluent monolayer of cells is by scratching a pipette over the surface, removing a strip of cells mechanically [5]. This technique is usually performed in wound healing assays, a simple practice for studying cell migration *in vitro*, allowing for monitoring of gap closure [3]. However, this technique has replications difficulties and often result in damaged cells surrounding the gap [6]. In addition, scratching do not provide the possibility to obtain gaps with specific geometries and sizes [7]. Consequently, other methods to generate gaps within a confluent layer of cells have been developed [8]. However, these methods have limited flexibility of forming gaps with arbitrary size and geometry.

This paper provides an introduction to cell migration, wound healing assays and the Biopixlar technology developed at Fluicell AB. In particular, gaps with different geometries and sizes formed in a confluent monolayer of cells using Fluicell's proprietary technology are presented. Finally, gap closure results of small gaps and large gaps are presented and discussed in relation to the initial area of the gap and inhibition conditions.

1.1 Background

This section presents background about current methods available for gap formation in cell layers and cell migrations assays. Subsequently, the importance of cell adhesion for gap closure is reviewed. Finally an overview of the Biopixlar technology, utilised in the project, is presented.

1.1.1 Cell migration and wound healing assays

Cell migration is a dynamic process essential for the function and development of multi-cellular organisms [9]. It is defined as the movement of cell clusters, sheets or individual cells and its absence has been associated with several pathological disorders in living organisms [10]. The cell migration process is affected by several

parameters, and the following categories are suggested as main influences: extracellular matrix (ECM) properties, cell-to-cell interactions, soluble factors, and cell autonomous properties [9]. The most common procedure *in vitro* for studying collective cell migration is the wound healing assay [9]. In basic steps, a wound healing assay involves formation of a gap in a monolayer of cells followed by capturing of images during the closure of the gap. Comparing the gap closure later allows for quantification of migration of cells [11]. An example of a cell-free gap is shown in Figure 1.1. In the most common assay, a gap is introduced by scratching a pipette tip over a confluent layer of cells, allowing surrounding cells to migrate into the gap space [3]. However, this assay has the downside of replication difficulties, but also in terms of damaged cells and ECM due to the mechanical scratch required to obtain the wound [6]. In addition, there are other methods to generate gaps within a confluent layer of cells, for instance, chemical and thermal removal [8]. These methods can obtain gaps of several geometries for studying cell migration [12]. For cell migration studies, rectangular and circular voids are favored [9] but studies of triangles and other arbitrary geometries have also been carried out [13] [12] [14]. However, the overall methods available for removal of cells from a confluent layer of cells to form gaps have limited flexibility in terms of shape and geometry.

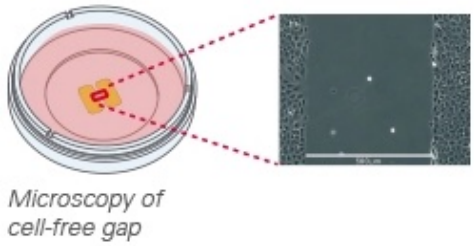

Figure 1.1: Cell-free gap in a dish filled with medium and the corresponding microscopy image of the gap. Image obtained and modified with permission from Ibidi [15]

Cell migration assays are relevant for inferring skin cells behaviour in skin wound models. Epithelial superficial wound closure is influenced by the migration of epithelial cells [16], and several studies have been performed covering epithelial cells in wound closure [17][18][19]. After skin wound formation, keratinocytes in the skin are partly responsible for the closure of the gap [20] and delayed migration of these cells has been shown to be related to delayed wound closure [21]. Keratinocytes are, among other cell types, important for restoring the structural properties of the skin [22]. To study mechanisms of gap closure *in vitro*, using primary keratinocytes have been suggested. However, the short lifespan of primary keratinocytes causes limitations of the inherent properties of the cells, compared to the immortalized human keratinocyte cell line (HaCaT) with a similar phenotype [23]. In addition, HaCaT cells have shown greater proliferation potential compared to normal human keratinocytes and do to not require the presence of growth factors in the medium during cell cultivation [24]. Furthermore, HaCaT has been extensively studied in wound healing and has been shown to be an appropriate keratinocyte model [25].

Finally, wound healing assays comparing HaCaT and normal human epithelial keratinocytes (NHEK) have shown greater wound closure for HaCaT without the addition of growth or differentiation factors [26] [27]. Because of these reasons, the HaCaT cell line was regarded as the best choice for a robust gap closure assay representative of a wound healing model.

Gap closure *in vitro* has been shown to consist of a combination of cell migration and proliferation [28]. To be able to measure cell migration *in vitro* and suppress cell proliferation, serum starvation before or after gap formation has been suggested [29]. Serum starvation has been performed *in vitro* before [30], however, it has been shown to have unpredictable effects on the cell cycle [31]. In addition, complete prevention of cell proliferation by serum starvation may be difficult; therefore, pretreatment of cells with substances such as mitomycin C has also been proposed [29]. Mitomycin C functions as a crosslinking agent and has been used in cancer therapy [32]. Planar rings on the molecule can be activated by photon-mediated cyclo-reduction or activation, attacking DNA bases on opposing strands. These crosslinks prevent DNA separation, thus inhibiting both DNA replication and transcription [33]. Consequently, inhibiting cell proliferation with mitomycin C was decided to be the best alternative for developing a gap closure assay of HaCaT cells.

Standard wound healing assays usually only study one specific initial wound shape, however one recent study has shown wound closure rates to be dependent on the initial wound shape. Here, the authors measured the area of the wound over time for square, circular, and triangular wounds and concluded the rate of closure to be dependent on the initial shape [34]. Furthermore, a study investigating cell movement in circular, triangular and rectangular shapes has shown wound closure to begin along the edges [35] and epithelial gap geometry has been shown to affect the closure of the gaps both *in vivo* and *in vitro* [13].

1.1.2 Cell adhesion

Cell adhesion *in vitro* is fundamental for tissue maintenance and development and is defined as the ability of one cell to hold on to another cell or an ECM substrate [36]. The composition of the ECM, and in particular the collagen content, has been shown to have importance for cell adhesion [37]. In addition, ECM biomaterials have been proposed as a component of bioinks [38], and decellularized ECM has been shown to contain several cell adhesive proteins [39]. Also, various types of coatings have become popular for improving the biological properties of materials and surfaces [40]. Both poly-l-lysine (PLL) and poly-glutamic acid (PGA) have been shown to increase cell adhesion to scaffolds [41]. However, PLL at too high concentrations has been shown to be toxic to cells, possibly due to cell membrane fusion [42].

Fibronectin (FN) is a multidomain glycoprotein commonly found in the blood and the ECM of different tissues [43]. It has been shown to affect the adhesion of several cell lines [44], and it has been suggested to affect epithelial migration in animal studies [45]. Furthermore, *in vivo* studies indicate that FN promotes epithelial

migration in the cornea [46]. Since the structure of the cornea shares similarity to that of skin, it is reasonable to believe that FN can have an enhancing effect on migration of keratinocytes. Early studies show FN-coated surfaces, enhancing keratinocyte migration *ex vivo*, suggesting fibronectin as a potentially important factor in wound healing therapies *in vivo* [47]. Therefore, studying how FN on the surface affects gap closure of HaCaT cells *in vitro* is of interest and will be considered in this study.

1.1.3 Biopixlar technology

In this study Fluicell's proprietary technology was utilised for gap formation in a confluent monolayer of cells. Therefore, this section will provide a general overview of the technology based on microfluidic technology, called Biopixlar. Biopixlar is a bioprinter with unique possibilities for depositing cells or molecules with high precision and resolution. The technology avoids the use of bioinks, making it suitable for the generation of multicellular biological tissues with direct cell-to cell contact [48]. It has several benefits compared to other existing bioprinting techniques. Biopixlar allows for generating patterns with arbitrary geometry with high precision [49] and without changing the printhead the technology enables printing of up to three different cell types. Furthermore, the printing process has been shown to not affect cell viability. With the fluorescence imaging setup, the technology also offers great possibilities to monitor the printing process in real time [50].

The Biopixlar technology employs a recirculating flow, enabled by the usage of a microfluidics-based printhead [51]. The pipette tip, fabricated in PDMS, contains eight different wells, also referred to as chambers, that can be pressurized. A schematic of the printhead is shown below in Figure 1.2

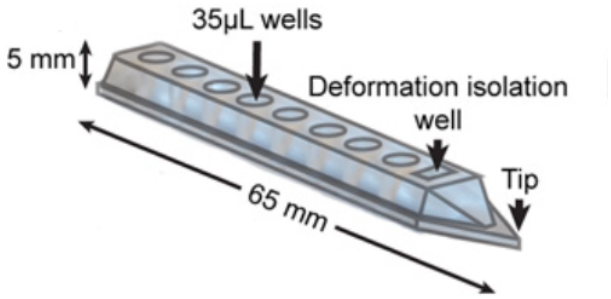

Figure 1.2: Schematic of the PDMS pipette used in the Biopixlar technology. Each well is connected to the tip through channels allowing pressure control. Figure modified and obtained from [51]

By controlling the recirculation zone, cells that do not adhere to the surface after deposition from the printhead are recirculated back into the pipette due to vacuum pressures from separate channels [48]. Figure 1.3 below show the key components

employed by the Biopixlar technology. In (a) the printhead is shown, allowing for printing of multiple cell types or molecules. In (b)-(c), fluorescence and bright-field images of the microfluidic channels of the printhead are shown. The recirculation flow of the tip can be adjusted by changing the pressures. The tip of the printhead is translated over the surface, allowing for printing of specific patterns, shown in (d)-(e). The delivery channel, placed in the middle of the tip of the printhead, is surrounded by vacuum channels providing negative pressures, thereby keeping cells refined to the recirculatory flow until interacting strongly enough to attach to the surface [48]. To facilitate printing, the Biopixlar bioprinter is combined with a software and a gamepad. The software allows for adjustment of camera settings, rate of printing and cell type. The gamepad interface generates the possibility of positioning the printhead as desired and printing cells.

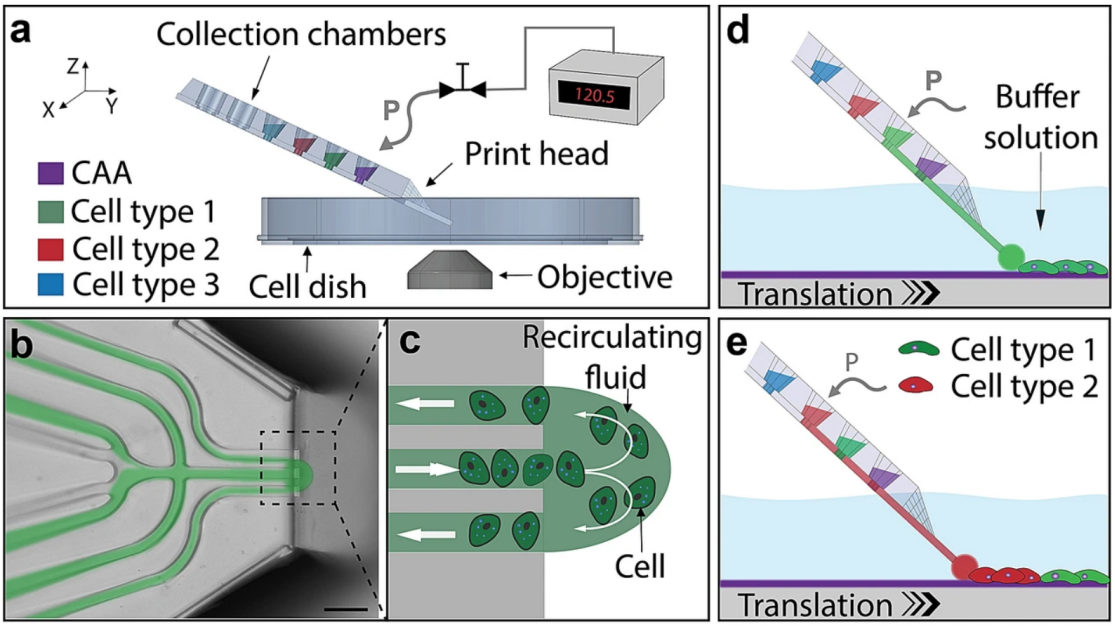

Figure 1.3: (a) An overview of the printhead and its key components. (b-c) An illustrative overview of the microfluidic channels of the printhead. (b) Fluorescence and bright-field images, showing the flows of the printhead. (c) The tip of the printhead indicating the recirculation zone. (d-e) Showing the usage of several cell types and agents. (d) By positioning the printhead close to the surface of a substrate within a buffer solution, cells are allowed to interact and attach to a localised region. (e) Changes in pressure within the tip allow multiple cell types to be printed without the need to move or replace the tip within the Biopixlar. Figure obtained from [48].

The main component of the Biopixlar is the microfluidic printhead. The printhead consists of four delivery chambers, illustrated in blue, green, yellow and red in Figure 1.4. Similarly, the four waste chambers are shown and illustrated in pink and orange. For printing molecules and cells, there is a need to add pressure to a delivery chamber. Thereupon, the solution in the chamber is pushed through the microfluidic channel towards the printing zone, exiting at the front of the printhead.

Unattached cells, together with residual liquid, are aspirated back into the channels of the printhead, illustrated in pink in Figure 1.4, and collected in the waste chambers indicated with pink colour. This process is of importance for maintaining the printing zone and ensuring that the printed solution is not diffused into the printing liquid. The orange channel (switch) ensures only the solution desired to print reaches the printing zone. Potential liquid coming out from other delivery chambers, will be aspirated back into the orange waste chambers, before reaching the printhead.

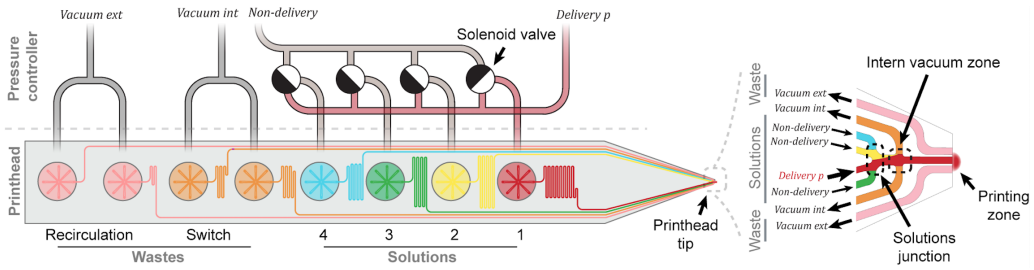

Figure 1.4: The microfluidic printhead. The printhead uses four chambers for delivery (blue, green, yellow, and red), through which solutions are pushed to the printhead upon pressurization. Four chambers are dedicated to waste collection (pink and orange). Potential liquid coming from the chambers not intended to use for printing is aspirated back into the orange chambers, and the unattached printing solution is collected back into the pink channel and chambers. Figure obtained from Shijun Xu at Fluicell AB.

1.2 Aim

The aim of the project is to use open-volume microfluidics to develop an *in vitro* gap-closure assay. Producing gaps with different geometries in a confluent monolayer of mammalian cells will allow for time-dependent gap closure to be monitored and analysed.

1.3 Goals and demarcations

The goals of the project is to develop protocols for the construction of gaps with geometric variance in a confluent layer of cells. Furthermore, analysing the cell behavior and cell viability of the cells upon the gap closure will be examined. Additionally, one of the objectives of the project is to learn relevant methods and acquire skills, including bioprinting, cell culturing, aseptic technique, microscopy imaging, and data analysis.

The study will be limited to the study of HaCaT cells, an immortal keratinocyte cell line, *in vitro*. Cell behaviour will be analysed in terms of cell count, following

inhibition of proliferation with mitomycin C. In addition, gap closure of gaps with different initial geometry and size will be analysed by imaging at predetermined time points. Finally, the attachment of fibronectin within gaps will be studied.

2
Methodology

This section will provide information about the materials and methods used during the experimental part of this study. Initially, the methodology of cell culturing and seeding will be presented followed by initial studies of cell proliferation inhibition performed with mitomycin C. Subsequently, sizes and geometries of gaps obtained in this study are presented. Finally, methods for gap closure conducted under cell proliferation inhibition together with procedures for measuring cell viability and attachment of fibronectin after gap formation are presented.

2.1 Cell culturing and subculturing

For the project, HaCaT (AddexBio, Cat: T0020001) were subcultured according to Fluicell AB protocols, between passages 20 and 41. Cells were cultivated in T25-flasks at 37°C, 5 % CO_2, and passaged when reached a confluency of 70-80 %. During cell culturing, cells were kept in dulbecco's modified eagle's medium high glucose (DMEM/basal media) (Sigma Aldrich, Cat: D5796) with 10 % fetal bovine serum (FBS) (Gibco, Cat. No. 10500064), hereafter referred to as growth media. For subculturing, remaining growth media was removed and the cells were gently washed with phosphate-buffered saline (PBS) (1X) (Cytiva HyClone, Cat: SH30256.FS). Cells were harvested using 0.25 % Trypsin-EDTA (1X) (Gibco, Cat: 25200056) and incubated at 37°C and 5 % CO_2 until detaching from the surface. 10-20 % of the cell suspension was then transferred to fresh growth medium, acclimatized at 37°C, and allowed to grow. When the cells had reached a confluency of 80-90 % the procedure was repeated.

2.2 Cell counting and seeding

Detachment of cells was followed by counting using a Bürker chamber and the desired number of cells was diluted in growth medium. For initial studies seeding was performed in a 12-well plate, further explained below in 2.3 Inhibition of cell proliferation with mitomycin C. For experiments aiming for gap formation and monitoring gap closure, 35 mm plastic petri dishes (Ibidi, Cat: 80156) were used for seeding. 40 000 cells mixed in growth media were seeded within the inner circle of the petri dishes. The dishes were cultured in incubation at 37°C and 5 % CO_2 until a fully confluent monolayer of cells was obtained, approximately for 72 hours.

2.3 Inhibition of cell proliferation with mitomycin C

This project aims for studying cell migration during gap closure. Therefore, to be able to measure migration of cells during gap closure there was a need to inhibit proliferation of cells. Mitomycin C has been shown to inhibit DNA synthesis by forming cross-links between adenine and guanine [52] thereby inhibiting cell proliferation. In earlier studies, inhibition of proliferation for wound healing assays have been performed with both serum starvation and exposure to mitomycin C, which was reviewed in 1.1.1 Cell migration and assays. Because of this, the projected initially focused on inhibition of cellular proliferation for HaCaT cells with mitomycin C in a 12-well plate. This was performed to study how cells in wells were affected upon mitomycin C exposure combined with basal or growth media, respectively. Inhibition conditions for mitomycin C were chosen according to literature [29][30].

20 000 HaCaT cells were seeded with growth medium in each well in a 12-well plate, to obtain an under-confluent culture (confluency of 5-10 %) which could be monitored for proliferation rates. Three areas of interest were marked in each well and imaged at time zero with bright-field microscopy using a 10X objective. Remaining growth media was then removed and all wells were washed gently with PBS twice to remove all traces of FBS. To investigate the impact of this inhibition (Sigma Aldrich, Cat: 10107409001), PBS was replaced with 5 μg/mL of mytomycin C (stock solution, 1 mg/ml) resuspended in basal media, according to the first two rows in Table 2.1 below. The controls, corresponding to the two bottom rows, were instead replaced with new basal or growth media. The 12-well plate was placed in incubation at 37°C and 5 % CO_2 for two hours. After incubation, all wells were washed with PBS twice to remove all traces of mitomycin C and new media was added according to the final column in Table 2.1. All wells were imaged (2h) before being placed in incubation until imaging time points 24 and 44 hours. The number of cells in these images were counted manually using Fiji software. Each condition was repeated in three wells and the experiment was repeated twice.

Table 2.1: Media conditions for the inhibition of HaCaT proliferation with mitomycin C in a 12-well plate. The conditions correspond to conditions in the cell count study performed, which results are shown in Figure 3.1. The two bottom conditions correspond to controls without inhibition of proliferation.

Cell count study		
Condition	Inhibition media	Media after inhibition
1	Mitomycin C + Basal media	Basal media
2	Mitomycin C + Basal media	Growth media
3	Growth media	Growth media
4	Basal media	Basal media

2.4 Gap dimensions

After initial studies of proliferation inhibition, the study moved on towards gap formation using Fluicell's proprietary technology. Initially, schematic drawings of gaps with different dimensions were formed. The size and geometry of gaps were based on earlier studies, reviewed in 1.1.1 Cell migration and assays. Some of these studies showed gap closure rate to be dependent on the initial geometry of gaps with square, triangular and circular shape (approximately 1000x1000 μm). Simultaneously another study, also reviewed in 1.1.1 Cell migration and assays, showed gap closure to be curvature-dependent (approximately 100x100 μm). Consequently, there was an interest in studying gaps with geometries as squares and circles, but also geometries with curvature, such as crescent moons. In addition, obtaining gaps with different size were of interest. Therefore, this section includes the geometries of the different gaps formed within this project. First, the different geometries of small gaps are shown, followed by larger gap geometries.

2.4.1 Small gaps

Initially, circular, square, and crescent moon-shaped gaps were formed on all dishes separately, according to Figure 2.1. The three gaps of approximately 300x300 μm were separated by a minimum of 1 mm. The square was 300x300 μm, the circle had a diameter of approximately 340 μm and the crescent moon was formed to obtain a total area similar as the other two geometries.

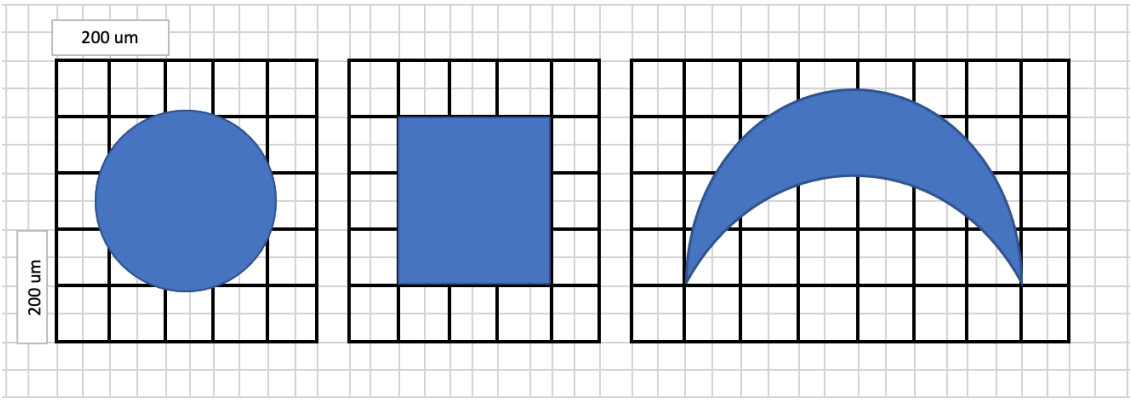

Figure 2.1: Schematic drawing for the geometries of small gaps intended to be formed with the Biopixlar technology. A circle, square and crescent moon, all with similar areas. Geometries were designed in Microsoft Excel.

2.4.2 Large gaps

Large square gaps were formed to obtain more time points of gap closure. Due to the short time limit of the project, large gaps with circular and crescent moon geometry were not formed. The square gaps were approximately 1000x1000 μm and were separated by a minimum of 2 mm.

2.5 Gap formation procedure

2.5.1 Cell proliferation inhibition with mitomycin C prior to formation of small gaps

Earlier in 2.3 Inhibition of cell proliferation with mitomycin C, Table 2.1 showed conditions selected for the initial study of cell count after exposure to mitomycin C. Based on the results from this study, presented in 3.1 Inhibition of cell proliferation with mitomycin C, three of these conditions were selected for monitoring gap closure. Since one aim of the project was to measure solely migration of cells, conditions inhibiting proliferation, but not migration, were first prioritised. Therefore, gap formation and gap closure of small gaps were conducted under conditions of inhibited proliferation. The inhibition media and media after formation of small gaps for the different conditions are shown in Table 2.2. Dishes with conditions 1-2 were inhibited with 5 μg/mL mitomycin C diluted in basal media for two hours. After inhibition, all dishes were washed with PBS twice and media were added according to the final column in Table 2.2. Dishes with condition 3 were controls and therefore not inhibited with mitomycin C but instead cultured in growth media.

Table 2.2: Media conditions for the inhibition of cell proliferation with mitomycin C before and after gap formation of small gaps. Condition 1-2 were exposed to mitomycin C (5 μg/mL) diluted in basal media for two hours. Condition 3 correspond to the control, without inhibition of proliferation. These conditions correspond to conditions utilised for studying gap closure of small gaps, presented in 3.3 Miniature gaps with different geometry.

Media composition before and after gap formation		
Condition	Inhibition media	Media after gap formation
1	Mitomycin C + Basal media	Basal media
2	Mitomycin C + Basal media	Growth media
3	Growth media	Growth media

Following proliferation inhibition with mitomycin C, gap formation with Fluicell's proprietary technology was performed according to gap dimensions in 2.4.1 Small gaps. However, gap closure for these gaps, presented in 3.3.1 Small gaps, led to further gap formation of larger gaps to be conducted without inhibition of proliferation. Therefore, gap closure of large square gaps, performed according to dimensions in 2.4.2 Large gaps, was solely performed for condition 3 from Table 2.2, thus conducted under conditions allowing a combination of migration and proliferation. Gap closure results for large square gaps are further presented in 3.3.2 Large gaps.

2.5.2 Attachment of fibronectin-FITC

As previously mentioned in 1.1.2 Cell adhesion, fibronectin has been shown to increase cell adhesion and promote cell migration. After gap formation of large square gaps, there was an interest in studying how fibronectin on the surface affect gap closure of HaCaT cells. To study this, initial tests of printing FN-FITC on a plastic surface without any cells were performed. Subsequently, printing FN-FITC after gap formation of large square gaps was performed. Fluorescein isothiocyanate (FITC) is often used for labeling proteins [53], peptides, antibodies and several other molecules [54]. In fibronectin-FITC (FN-FITC), FITC is conjugated to fibronectin via primary amines [53]. Therefore, FN-FITC is fluorescent and can be visualised both when printing and in fluorescent microscopy.

To study the attachment of FN-FITC (Sigma Aldrich, Cat: F2733-1ML) initially, a working solution of 0.5 mg/ml [w/v] FN-FITC in PBS was prepared and placed in a delivery chamber of the printhead. The solution was printed on plastic petri dishes without cells. The goal was to print lines on different locations in dishes filled with PBS, basal media or growth media, respectively. Immediately after printing, the efficiency of fibronectin attachment was imaged by fluorescence microscopy. In addition, printing FN-FITC after gap formation of large square gaps was performed. Immediately after gap formation, FN-FITC diluted in PBS at a concentration of 0.5 mg/ml was placed in the printhead and printed over the gaps. This was tested solely for large square gaps. The efficiency of the attachment was imaged in fluorescence microscopy immediately after printing.

2.5.3 Viability assay

Live dead staining was performed using fluorescein diacetate (FDA) (Sigma Aldrich, Cat: F7378-5G, stock: 5 mg/mL) and propidium iodide (PI) (Sigma Aldrich, Cat: P4170, stock: 2 mg/mL) combined with Hoechst staining (Fisher, Cat:H1399, stock: 10 mg/mL) to study the viability of cells after small gap formation. FDA is a dye that permeates membranes and gets hydrolysed, which leads to green fluorescence. Hence the cells that show positive and strong staining for FDA are viable cells. PI, however, binds to DNA by intercalating between nucleic bases, leading to a red shift of the excitation and emission maximum and an increase in fluorescence intensity. It is impermeable to cells with an intact membrane, thus cells showing strong staining for PI are dead cells. Hoechst 33342 is also a DNA dye used for nuclei staining, however staining living cells. It is cell-permeable and upon binding to DNA strands blue fluorescence is greatly enhanced.

A staining solution was prepared with basal media mixed with FDA, PI, and Hoechst 33342 in 1:625, 1:100 and 1:1500 dilutions, respectively. Two hours after gap formation, all cell media from dishes were removed and the staining solution was added for 5 minutes at incubation at 37°C and 5 % CO_2. The staining solution was then removed and the samples were washed twice with PBS before basal media was added. The dishes were then visualised and imaged using fluorescence microscopy

and bright-field microscopy. The purpose of viability testing was to confirm the Biopixlar technology can target and ablate only the desired area while producing the gaps.

2.6 Data acquisition and analysis

Dishes were studied in a LED fluorescence microscope (Zeiss Axiovert A1, Carl Zeiss, Germany) with 5x and 10x objectives. Images were captured by using a ZEISS Axiocam 305C by Zen Blue software. Bright-field microscopy images of the initial gap immediately after gap formation were taken and considered as time zero. By studying the area of the gap during several following time points (0, 4 and 22 hours for small gaps; 0, 22, 28 and 44 hours for large gaps) the rate of gap closure for each gap could be assessed. Image processing was done with Fiji software. The edges were sharpened and a threshold was set, making cells appear as white and clear gaps as black. Following, the freehand selection or wand (tracing) tool was used in Fiji software for making yellow lines surrounding the gap. An example of this process for large square gaps is shown in Figure 2.2. By setting a threshold, the software could distinguish between the gap and the surrounding cells. The size of the gaps could then be calculated in the software and the percentage of gap closure for each time point could be obtained by normalising the gap area by the initial gap area.

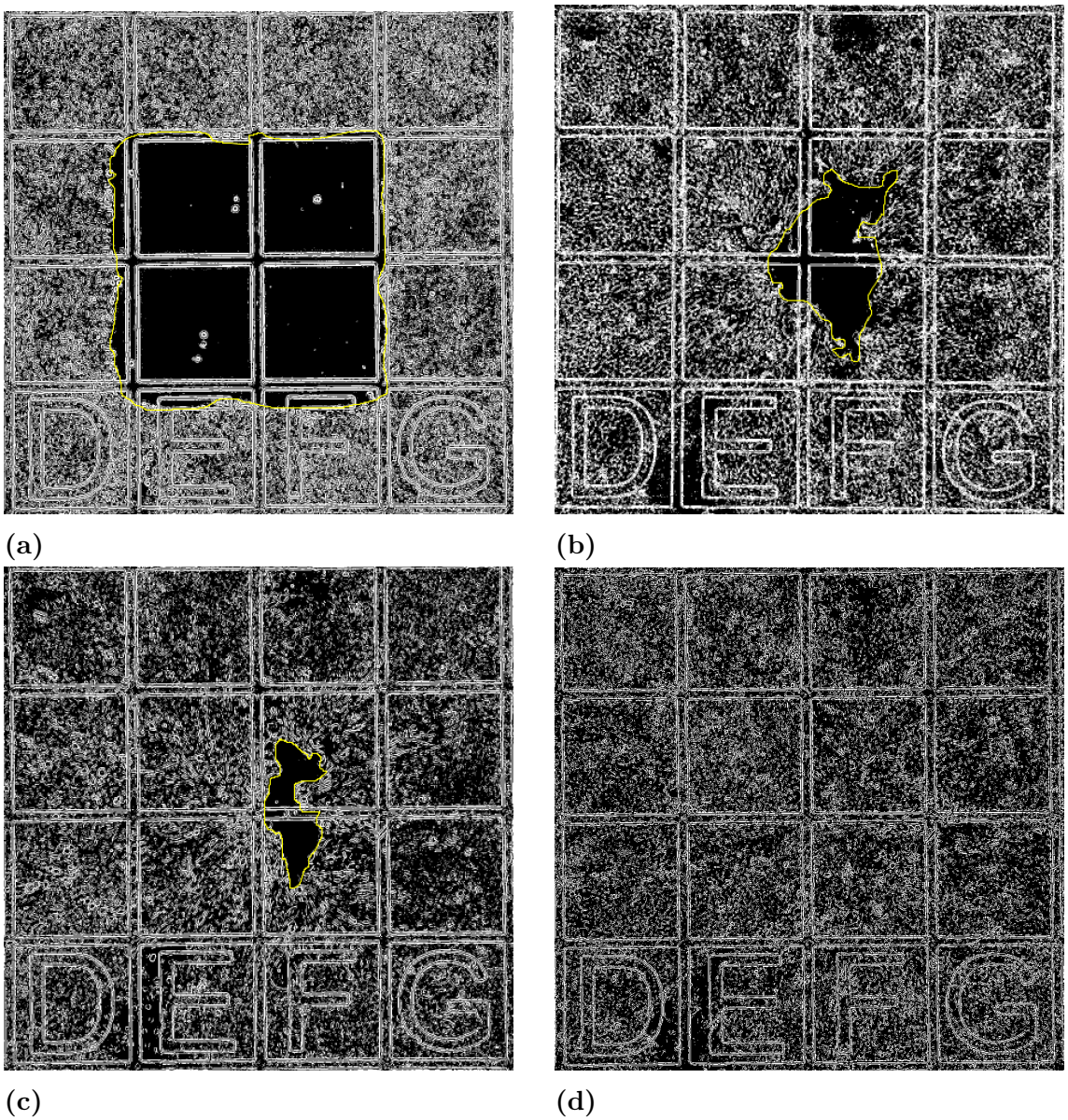

Figure 2.2: 5X bright-field microscopy images gap closure for large square gap in a confluent monolayer of HaCaT cells. The figures illustrates image processing performed with Fiji software for studying gap closure. Cells appear as white and gaps as black. Yellow lines surrounding the gap were added manually or automatically for calculation of the gap area. Gap was monitored during time points (a) 0 hours, (b) 22 hours, (c) 28 hours, and (d) 44 hours.

Quantitative holographic phase microscopy was performing using a Holomonitor M4 (Phase holographic imaging, PHI AB). Data was acquired and processed using the Hstudio suite (Phase holographic imaging, PHI AB). The technology allowed for the comparison of the height profile for gaps.

3
Results

This section describes results from the initial inhibition of cell proliferation and the viability studies after gap formation. In particular, it demonstrates gap closure of gaps with different sizes and geometries, formed with Fluicell's proprietary technology. Finally, the results of printing FITC-fibronectin in different media compositions are presented.

3.1 Inhibition of cell proliferation with mitomycin C

Initially the impact of inhibition with mitomycin C on HaCaT cell count was studied using a 12-well plate. The goal was to achieve conditions with inhibition of cell proliferation, thereby allowing for studies of solely cell migration. Cell count was defined as the number of cells within a specific area, and compared between imaging time points (0, 2, 24 and 44 hours). The number of cells for time points 4, 24 and 44 hours were normalised based on the initial amount of cells (0 hours) and the average cell count for each condition after normalisation is presented below in Figure 3.1. The cell loss after 44 hours was more than 50 % for both conditions (1-2) exposed to mitomycin C during inhibition. Conditions were selected according to Table 2.1. The controls (condition 3-4), also shown in Table 2.1 were not exposed to mitomycin C but instead kept in growth or basal media, and showed increased number of cells after both 22 and 44 hours. All four conditions were repeated in three wells, respectively, and the experiment was repeated twice.

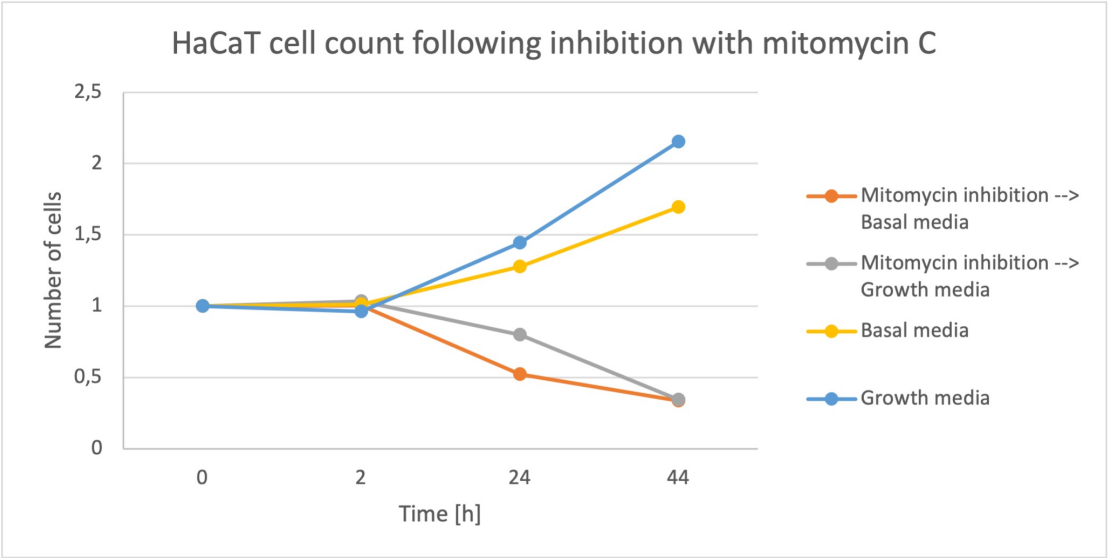

Figure 3.1: Cell count of HaCaT cells in a 12-well plate during and after mytomycin C inhibition, in comparison to controls without inhibition. The number of cells were normalised based on the initial amount of cells in the area. Orange (condition 1) and grey (condition 2) data points correspond to wells being exposed to mitomycin C inhibition for two hours and later kept in basal or growth media. Yellow (condition 4) and blue (condition 3) data points correspond to cells being cultured in basal or growth media at all times.

Both condition 1 and 2 (orange and grey) in Figure 3.1 show decreased cell count after both 22 and 44 hours. The DNA synthesis of cells in these conditions is inhibited, thus proliferation is not continuing after exposure to mitomycin C. These conditions therefore provides the possibility to measure solely cell migration when monitoring gap closure. Since the controls (condition 3-4, blue and yellow) show increased cell count, cell proliferation continues in both basal and growth media without mitomycin C inhibition. At both 22 and 44 hours, cell count in condition 3 was higher compared to condition 4, indicating higher rate of proliferation. For the following studies, monitoring gap closure, experimental conditions obtaining inhibition of proliferation were prioritised, thus conditions 1-2 were chosen. In addition, one control condition (condition 3) were included for gap closure studies.

3.2 Formation of miniature gaps and cell viability

To test how gap formation affects remaining cells, staining with FDA, PI and Hoechst 33342 was performed. Viability assay was performed after gap formation for dishes with condition 1-3. Viability results were similar, both for conditions with (1-2) and without (3) mitomycin C inhibition. Hence, the gap formation procedure available using Fluicell's proprietary technology is able to form gaps with specific geometries while maintaining viability for cells surrounding the gap.

A representative result of the viability assay for a crescent moon gap is shown below

in Figure 3.2. In (a) a 5X bright-field microscopy image of a crescent moon gap modified by adding a yellow contour surrounding the gap is presented, followed by fluorescence microscopy images of the gap after staining with (b) FDA, (c) PI and (d) Hoechst 33342.

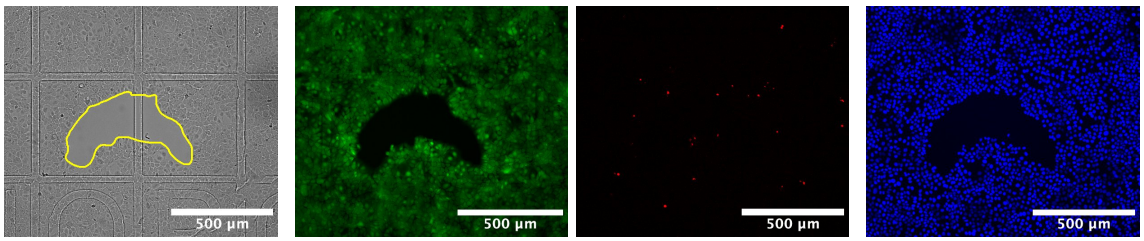

(a) **(b)** **(c)** **(d)**

Figure 3.2: 5X bright-field and fluorescence microscopy images of a small crescent moon gap after gap formation and washing with PBS. (a) Bright-field image modified by adding a yellow contour indicating the cells surrounding the gap. (b) Viable HaCaT cells emitting green fluorescence after staining with FDA. (c) Dead HaCaT cells emitting red fluorescence after staining with PI. (d) Nuclei of HaCaT cells emitting blue fluorescence after Hoechst 33342 staining. Scale bar = 500 μm.

Figure 3.3 show a representative result of the viability assay performed after gap formation of a square. In Figure 3.3 (a) a 5X bright-field microscopy image of a square gap modified by adding a yellow contour surrounding the gap is presented, followed by fluorescence microscopy images of the gap after staining with (b) FDA, (c) PI and (d) Hoechst 33342.

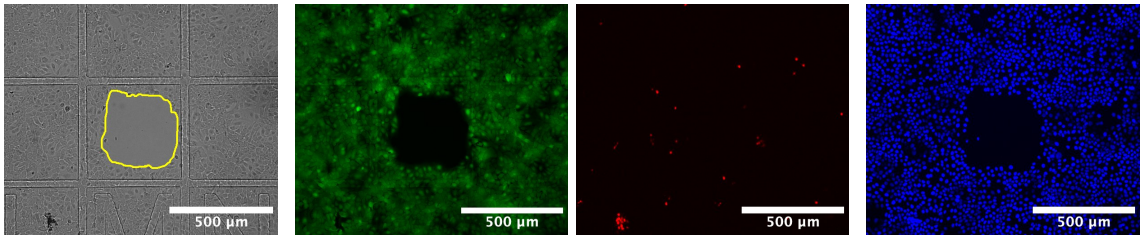

(a) **(b)** **(c)** **(d)**

Figure 3.3: 5X bright-field and fluorescence microscopy images of a small square gap after gap formation and washing with PBS. (a) Bright-field image modified by adding a yellow contour indicating the cells surrounding the gap. (b) Viable HaCaT cells emitting green fluorescence after staining with FDA. (c) Dead HaCaT cells emitting red fluorescence after staining with PI. (d) Nuclei of HaCaT cells emitting blue fluorescence after Hoechst 33342 staining. Scale bar = 500 μm.

In a similar way, in Figure 3.4 (a) a 5X bright-field microscopy image of a small circle gap is shown after modification by adding a yellow contour surrounding the gap, followed by fluorescence microscopy images of the gap after staining with (b) FDA, (c) PI and (d) Hoechst 33342.

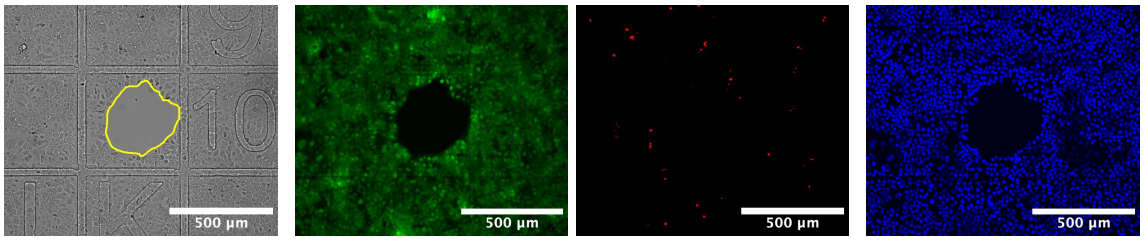

(a) **(b)** **(c)** **(d)**

Figure 3.4: 5X bright-field and fluorescence microscopy images of a small circle gap after gap formation and washing with PBS. (a) Bright-field image modified by adding a yellow contour indicating the cells surrounding the gap. (b) Live HaCaT cells emitting green fluorescence after staining with FDA. (c) Dead HaCaT cells emitting red fluorescence after staining with PI. (d) Nuclei of HaCaT cells emitting blue fluorescence after Hoechst 33342 staining. Scale bar = 500 μm.

In addition, Fluicell's proprietary technology allows for formation of gaps with very little to no cell debris. With phase contrast microscopy the height profile of gaps could be visualised. Below in Figure 3.5 an example of a crescent moon gap with a clear surface is shown. In the figure, the presented height profile show a difference of approximately 5.6 μm between the gap and the surrounding cells.

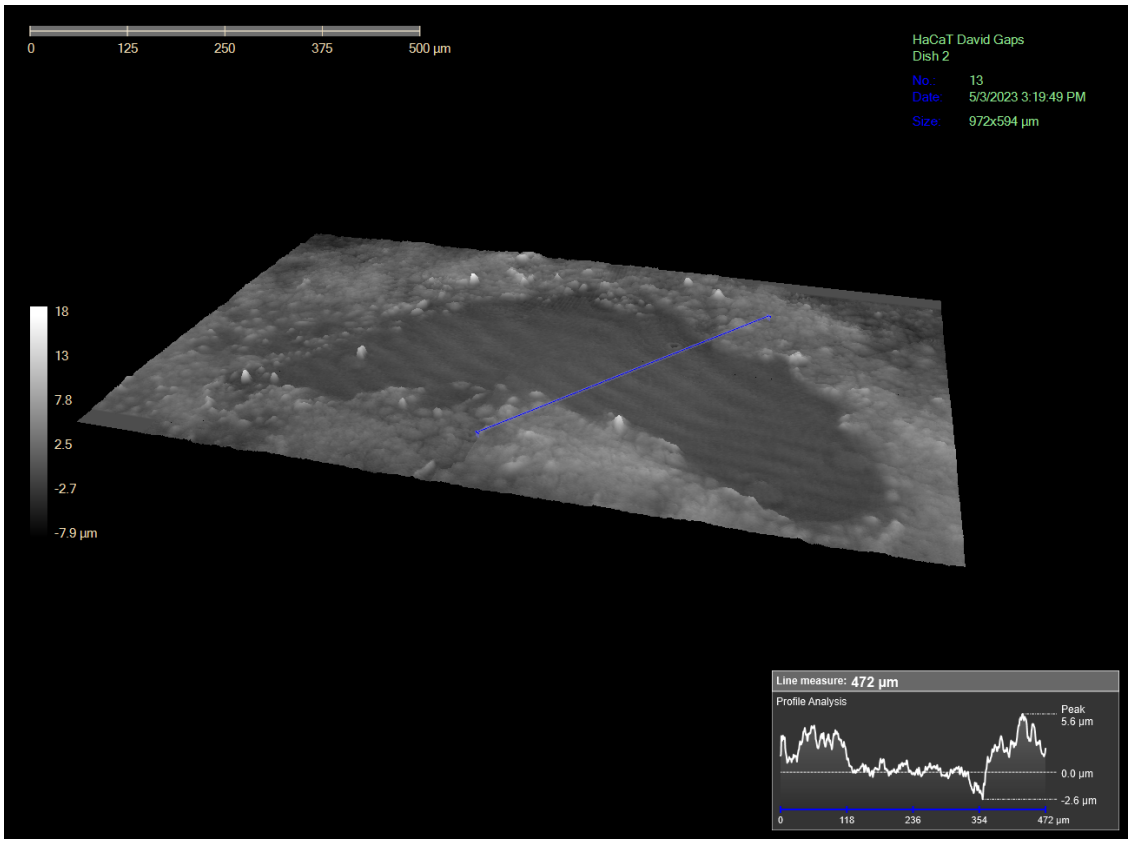

Figure 3.5: Phase contrast microscopy image of small crescent moon gap in a confluent monolayer of HaCaT cells immediately after gap formation. Imaging was performed using a Holomonitor M4 (Phase holographic imaging, PHI AB). Scale bar (upper left) = 500 μm. The obtained height profile is observered in the bottom right of the image and is based on the blue line over the gap.

3.3 Miniature gaps with different geometry

Gap formation was performed with Fluicell's proprietary technology and the gap closure was studied by imaging during several check-up points. Gap formation was performed for both small gaps (approximately 300 x 300 μm) and large gaps (1000 x 1000 μm). Small gaps were formed under conditions of inhibited proliferation with mitomycin C, while large gaps were formed under conditions of both migration and proliferation, since no mitomycin C inhibition was performed.

3.3.1 Small gaps

Gap closure for small gaps was conducted under conditions of no proliferation. Below in Figure 3.6 examples of gap closure for the three different shapes for time points 0-1, 4 and 22 hours are presented.

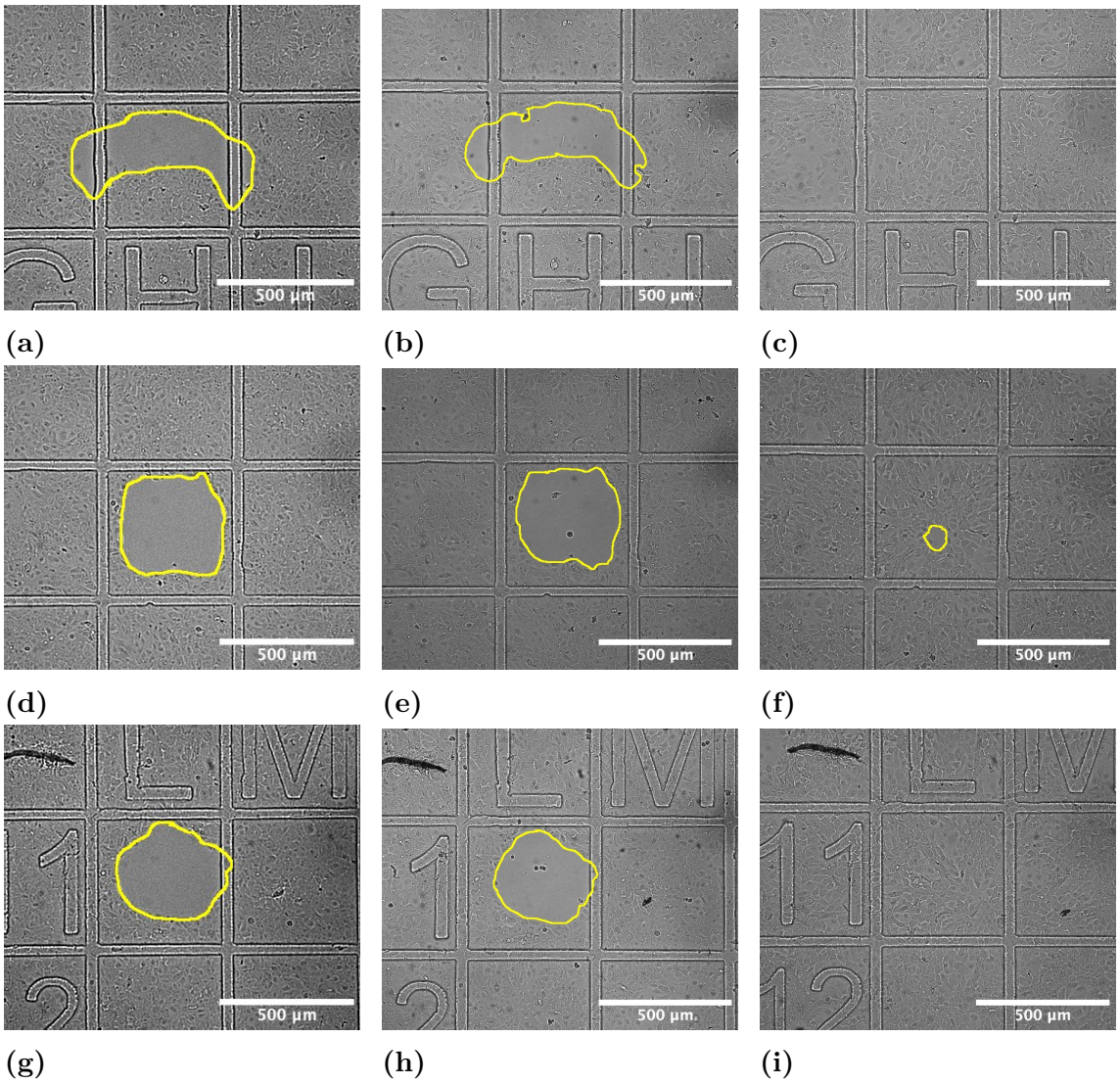

Figure 3.6: 5X bright-field microscopy images representing closure of a small gaps during time points 0-1 hours, 4 hours and 22 hours. Images were modified by adding a yellow contour surrounding the gap. When full closure was obtained, no yellow line was added. Intended initial geometry of the gap was (a)-(c) crescent moon, (d)-(f) square and (g)-(i) circle. Scale bar = 500 μm. Image modifications in Fiji software was performed for increasing the brightness.

Gap closure for small gaps was monitored under conditions shown in Table 2.2. Condition 1-2 correspond to proliferation inhibition with mitomycin C followed by addition of basal or growth media, respectively. Condition 3 correspond to a control condition, without inhibition of proliferation. The area for each gap was measured for each time point, according to the 2.6 Data acquisition and analysis, and the average gap closure for each time point was summarised into Figure 3.7. Full gap closure of the culture was defined as when no empty space was visible, meaning when cells were covering the complete area of the initial gap. The average gap closure for gaps monitored under condition 1 (a) was almost zero. This was due to gaps loosing the initial geometry upon gap closure, thus becoming even larger

at time points 4 and 22 hours. A representative image of gap closure for a square gap monitored under condition 1 is shown in Appendix A. Gaps in condition 2 (b) and 3 (c) show an increase in gap closure for both time points 4 and 22 hours. Full closure is reached after approximately 22 hours. The majority of the gaps imaged for condition 2 (b) and 3 (c) were completely closed after 22 hours, however some gaps showed significantly lower closure which is the reason for the average closure not being 100 %.

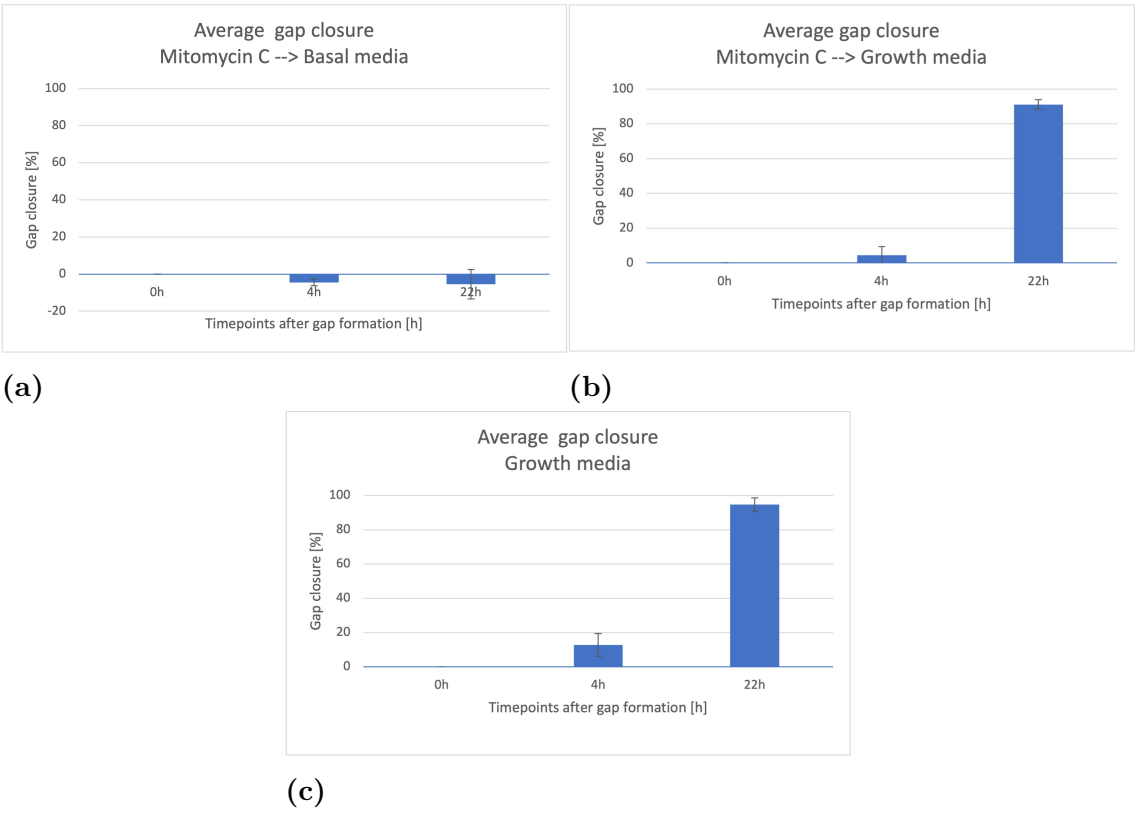

(a) **(b)**

(c)

Figure 3.7: Average HaCaT gap closure with time points corresponding to the time after gap formation. (a) Average gap closure after two hours mitomycin C inhibition followed by gap formation and culturing in basal media (condition 1), N=12. (b) Average gap closure after two hours mitomycin C inhibition followed by gap formation and culturing in growth media (condition 2), N=14. (c) Average gap closure after gap formation where dishes were cultured in growth media both before and after gap formation (condition 3), N=11, (N=technical replicates).

3.3.2 Large gaps

Closure of large gaps was conducted under conditions of both proliferation and migration to allow for full gap closure. In Figure 3.8 an example of gap closure for a large gap is presented. A square gap formed in a confluent layer of HaCaT cells was imaged at four time points (0, 22, 28 and 44 hours). Full closure of the gap was reached after 44 hours.

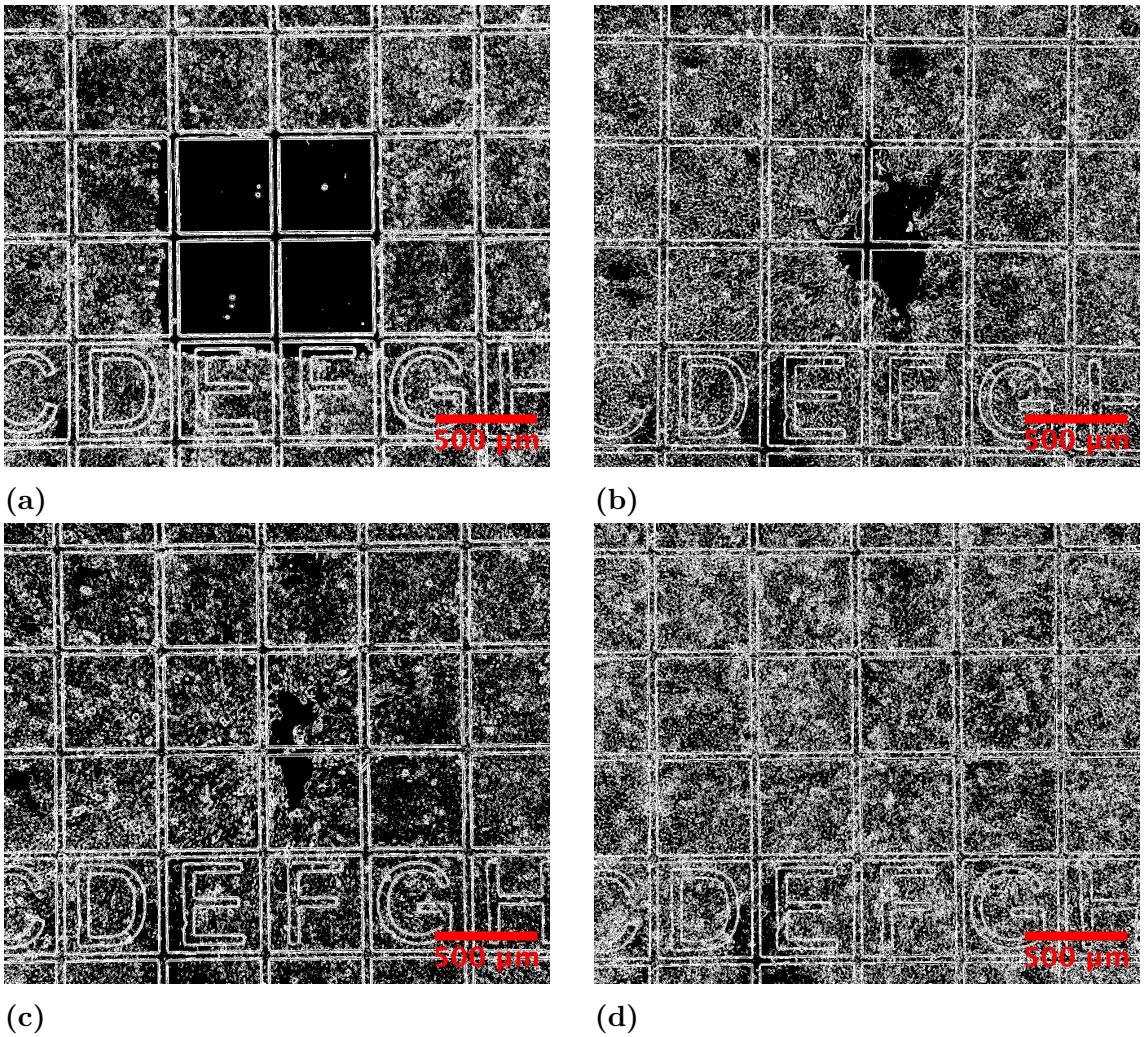

Figure 3.8: 5X bright-field microscopy images of 1000 x 1000 μm square gap in a confluent monolayer of HaCaT cells, during time points (a) 0 hours, (b) 22 hours, (c) 28 hours, and (d) 44 hours. Dishes were kept in growth media (condition 3) at all times. Image processing was performed in Fiji software. Scale bar = 500 μm.

The area of the gap was measured for each time point, and the average HaCaT gap closure of large gaps were summarised into Figure 3.9. More than 70 % of the initial area of the gaps were closed after 22 hours and full closure was reached after 44 hours. Full gap closure of the culture was, as for small gaps, defined as when no empty space was visible and cells were covering the complete area of the initial gap. Future studies will require monitoring gap closure by additional time points, which will be further explained in 4 Discussion, however doing so was beyond this study.

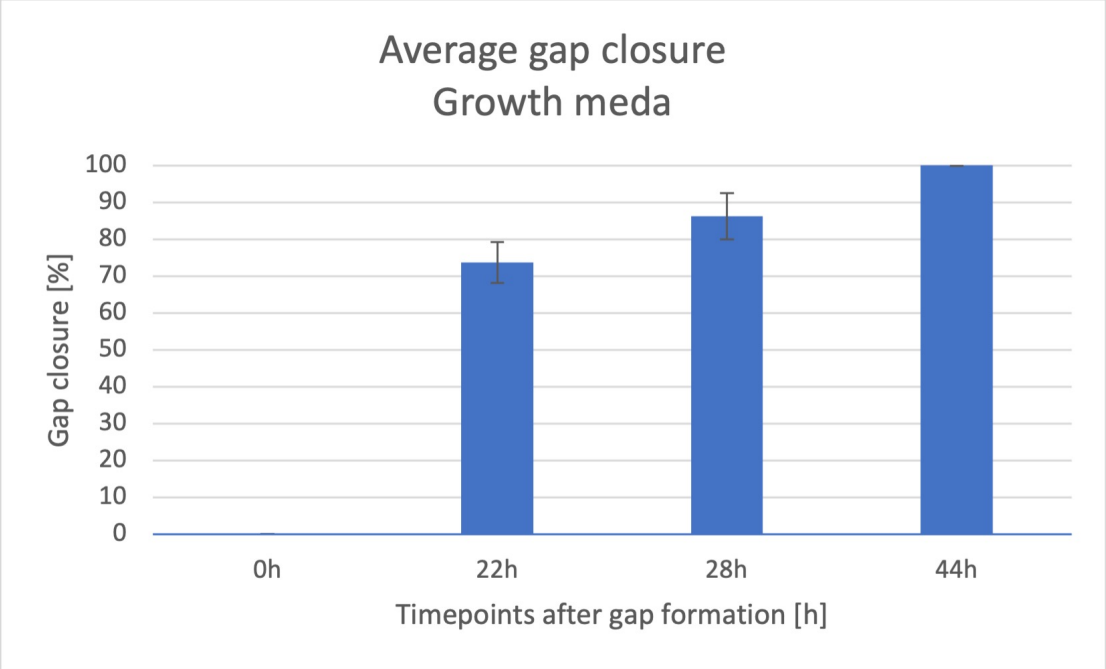

Figure 3.9: Average HaCaT gap closure for large square gaps under conditions of both proliferation and migration (condition 3), N=3. The area of the gaps were normalised based on their initial area.

3.4 Attachment efficiency of FN-FITC

Fibronectin is important for modulating cellular migration and adhesion during gap closure. Therefore, there was an interest in studying how fibronectin on the surface affect gap closure of HaCaT cells, thus attachment of FN-FITC when printing with the Biopixlar was studied. Figure 3.10 display images of fluorescence microscopy immediately after printing FN-FITC on regular plastic dishes without any cells, in both PBS and basal media, respectively. The figure shows the attachment of FN-FITC on a plastic surface in (a) PBS and (b) basal media. Image modifications in Fiji software was performed for increasing the brightness of the fluorescence.

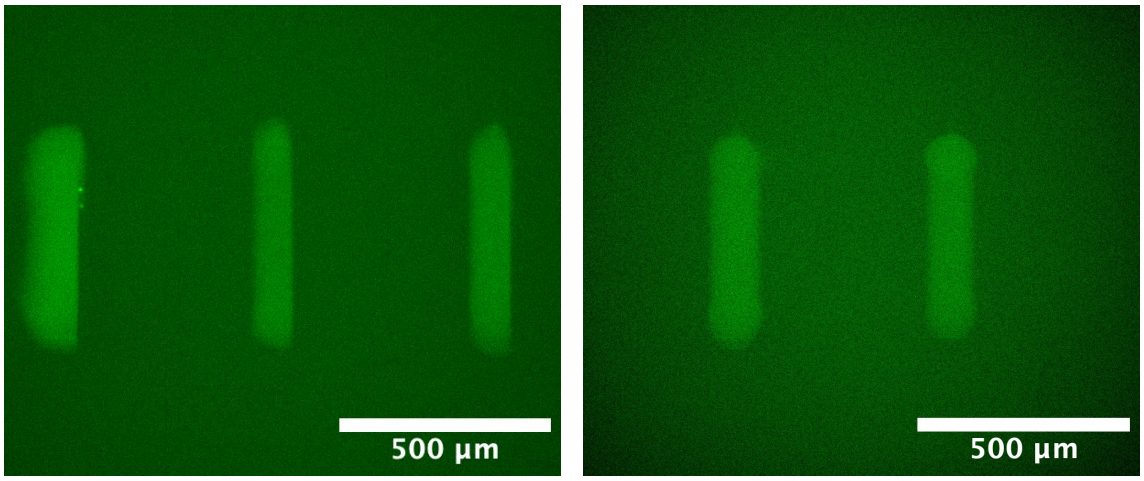

(a) **(b)**

Figure 3.10: 5X fluorescence microscopy images. Green fluorescence showing attachment of FN-FITC on plastic surface in a petri dish without cells, 0 hours after printing in (a) PBS and (b) basal media. Scale bar = 500 μm.

Printing FN-FITC on a plastic petri dish without any cells as well as in the gap areas after gap formation was not possible. Optimisation of bioprinting protocols for FN-FITC inside the gap regions require further optimisation, which was beyond this study.

4
Discussion

This section will provide an introduction to existing gap closure assays and common techniques for inhibiting cell proliferation. Subsequently, results of gap closure of miniature gaps are discussed in relation to results of inhibition of cell proliferation with mitomycin C. Furthermore, the results of printing fibronectin within gaps are analysed and finally potential error sources during the study are mentioned.

Wound healing is a complex biochemical and cellular process, necessary for tissue repair in living organisms [1]. Wounds *in vivo* exhibit a broad variety of geometrical shapes [55], and the closure rate has been shown to be affected by the initial geometry of the wound [55]. In addition, earlier studies showed gap closure of different geometries *in vitro* to be dependent on the initial shape of the gap [34][13]. Therefore, there was an interest in studying closure rate of gaps with different initial geometries *in vitro*. Established cell-removing methods are often simple, allowing for studying collective cell migration over cell-free areas [1] [3] [56]. However, scratch assays only allow for formation of lines, with a width usually smaller than 900 μm [9]. Other, more recently developed studies has allowed for studying gap closure of several geometries such as circles, squares and triangles [13] [14], but overall these methods have limited flexibility of forming gaps with arbitrary size and geometry. In addition, methods have not been performed for HaCaT cells with inhibition of cell proliferation using mitomycin C. On the other hand, scratch assays of HaCaT cells under conditions of inhibited proliferation have been performed earlier [29], though not for gaps with more complex geometries. The presented study provides an *in vitro* gap closure-assay of gaps with different initial geometries and sizes, formed using Fluicell's proprietary technology. The assay enable gaps formed in a confluent monolayer of HaCaT cells to be monitored under conditions where cells are allowed to proliferate and under conditions of no proliferation. Moreover, viability studies demonstrate viability of cells surrounding the gaps to be high after gap formation. Finally, this study also provides elemental observations of printing fibronectin-FITC within gaps.

Formation of miniature gaps were conducted under conditions of no proliferation and conditions of proliferation. Gaps in condition 1 (mitomycin C inhibition, gap formation, basal media), aimed for measuring cell migration solely, did not show any gap closure, see Figure 3.7 (a), supported by representative images in Appendix A Gap closure of small gaps monitored under conditions of no cell proliferation. This could possibly be explained by the reduced number of cells due to cell death, shown in Figure 3.1. Since almost 50 % of the cells died (based on the initial

cell count) for condition 1 after 24 hours, it is reasonable that the gap will not be able to close. Condition 2, in Figure 3.1, showed a similar loss in cell count as condition 1. However, gaps in condition 2 (mitomycin C inhibition, gap formation, growth media), also aimed for measuring cell migration solely, did almost show full gap closure, see Figure 3.7 (b). Condition 3, in Figure 3.1, aimed at providing a condition of proliferation, showed increased cell count after both 24 and 44 hours. Gaps in this condition also showed almost full closure, shown 3.7 (c).

In summary, according to Figure 3.1 and Figure 3.7 (a), mitomycin C results in reduced number of cells during the gap closure period. Simultaneously, Figure 3.7 (b) shows almost full closure of small gaps, despite mitomycin C inhibition prior to gap formation. Since the only difference between these two conditions ((a) and (b)) is the media after the gap formation, the growth medium seems to enhance the gap closure significantly. In earlier studies, HaCaT cells have been shown to be less proliferative when grown without serum than with serum [57], which could be one reason for this. If mitomycin C inhibition is able to fully suppress proliferation, gap closure monitored under condition 2 (b) would indicate successful migration of the gap. However, it is possible that inhibition was not entirely successful in terms of suppressing proliferation. This is supported by the literature, suggesting treatment in serum-free media to study cell migration [58], therefore, the closure of gaps conducted in condition 2 is potentially a combination of migration and proliferation. Condition 3 (Figure 3.7 (c)), the control, showed similar results as condition 2 (b), with only 8 and 4 % higher gap closure at time points 4 and 22 hours, respectively. This is reasonable, since Figure 3.1 shows increased cell count for condition 3 (growth media, gap formation, growth media), suggesting ongoing proliferation of cells during gap closure. On the other hand, other studies of gap closure conducted under conditions of proliferation, without addition of proteins to the media, did not show, or only showed little, gap closure [59] [29]. Concisely, mitomycin C inhibition results were inconsistent compared to those of the literature. This conclusion was a major reason for studying large gap closure without inhibition conditions. Instead of focusing on migration solely, the study moved towards investigating gap closure, under conditions of both migration and proliferation.

For small gaps, there was only one single time point between the initial gap and the fully closed one. Because of this it is possible full gap closure was obtained at an earlier time point. Due to this, the thesis moved on towards the formation of larger gaps, thereby obtaining more time points between the initial and fully closed gap, which is seen in Figure 3.9.

Attaching fibronectin to gaps was of interest to promote cell adhesion and migration during gap closure. Therefore, gap formation of larger gaps followed by printing FN-FITC within the gaps was performed. Growth media, containing DMEM and 10 % FBS, inhibited attachment on FN-FITC on plastic surfaces. Since all dishes aimed for gap closure studies were cultured in growth media it was not possible to conduct a study investigating the effect of fibronectin on gap closure. However, the attachment of FN-FITC on plastic surfaces was successful when printing in basal

media and PBS (Figure 3.10). One reason for this may be Bovine Serum Albumin (BSA), a major component in FBS [60]. BSA is widely used for surface passivation applications, aimed at minimising non-specific binding of biomolecules [61]. The protein has a negative charge [62], which has also been shown for FITC [63]. This similarity may suppress the binding of FN-FITC to the surface in the presence of growth media.

Finally, it is also important to mention possible sources of errors during the project. Since the image analysis software had difficulties of separating single cells and clusters when automatically counting cells, cell counting was performed manually. Manual counting of cells during data analysis, for Figure 3.1, can potentially lead to certain areas being over- or under-counted. This was addressed by having three data points for each well and calculating the average cell count after normalisation. In addition, the area of the gaps were mainly automatically calculated by the analysis software. However, when this was not applicable, due to cell debris or imaging quality, calculation was performed manually. Since the automatic calculation performed by the software could be more precise compared to the manual calculation, this could potentially lead to gap closure results being over- or underestimated. This was addressed by calculating the average gap closure, thus reducing the impact of this potential error source.

4.1 Future studies

This study provided time-dependent gap closure to be monitored and analysed. However, adding time points for both small and large gaps would improve analysis of gap closure. For small gaps, adding time points between 4 and 22 hours should be prioritised, while for large gaps, time points between 4-22 hours and 28-44 hours should be in focus. With an incubator microscope for live cell imaging, monitoring the gap at even more time points during closure would be possible.

Furthermore, difficulties observed when printing FN-FITC in growth media has been presented. To further study possible cell adhesion and migration promotion with fibronectin during gap closure, different paths should be considered. One route could aim for removal of surface proteins blocking the binding of fibronectin to the surface. This could potentially be performed by manual removal, for instance by scratching the surface, in basal media or PBS. In addition, another route could be finding a molecule, able to attach to the gap surface in growth media, that also enables fibronectin-FITC to be attached onto. This way fibronectin-FITC could be successfully printed within gaps.

In addition, additional studies on mitomycin C are of interest to better understand the behavior of HaCaT cells after inhibition of proliferation. Inhibition performed with lower concentration of mitomycin C, or for a shorter time period, would be initial tests to perform. In addition, complementary or supplementary serum starvation methods could be tested.

5
Conclusion

In conclusion, this study illustrates the possibility of using open-volume microfludicis to develop a gap closure assay with arbitrary geometry and size in a confluent monolayer of cells. Fluicell's proprietary technology provides the possibility to form gaps with no cell debris *in vitro* without affecting the viability of surrounding cells. The results demonstrated time-dependent closure of gaps with different geometries and sizes to be studied and analysed. Furthermore, gap closure was monitored under conditions of cell proliferation and no proliferation. For continuing studies of gap closure under conditions of cell migration solely, mitomycin C inhibition is a possible route, however further optimisation for HaCaT cells is necessary. In addition, for understanding the effect of fibronectin on gap closure, more studies on attachment efficiency of FN in different media composition is required. However, this study has highlighted both existing opportunities and challenges in studying the closure of gaps with different initial geometry. Overall, the project ad on to the current research field of gap closure assays and provides principal knowledge needed for future studies aiming towards formation of gaps with more complex geometries.

References

[1] Ayman Grada et al. "Research Techniques Made Simple: Analysis of Collective Cell Migration Using the Wound Healing Assay". In: *Journal of Investigative Dermatology* 137.2 (2017), e11–e16. ISSN: 0022-202X. DOI: 10.1016/j.jid.2016.11.020.

[2] Kristo Nuutila et al. "Human Wound-Healing Research: Issues and Perspectives for Studies Using Wide-Scale Analytic Platforms". In: *Advances in Wound Care* 3.3 (Mar. 2014), pp. 264–271. ISSN: 2162-1918. DOI: 10.1089/wound.2013.0502.

[3] James Jonkman et al. "An introduction to the wound healing assay using live-cell microscopy". In: *Cell Adhesion & Migration* 8 (2014), pp. 440–451. DOI: 10.4161/cam.36224.

[4] Anne Stamm et al. *In vitro wound healing assays - State of the art*. May 2016. DOI: 10.1515/bnm-2016-0002.

[5] Ester Anon et al. "Cell crawling mediates collective cell migration to close undamaged epithelial gaps". In: *Proceedings of the National Academy of Sciences* 109.27 (2012), pp. 10891–10896. DOI: 10.1073/pnas.1117814109.

[6] Jin Young Lin, Kai Yin Lo, and Yung Shin Sun. "A microfluidics-based wound-healing assay for studying the effects of shear stresses, wound widths, and chemicals on the wound-healing process". In: *Scientific Reports* 9.1 (Dec. 2019). ISSN: 20452322. DOI: 10.1038/s41598-019-56753-9.

[7] Shang Ying Wu et al. "A wound-healing assay based on ultraviolet light ablation". In: *SLAS Technology* 22.1 (Feb. 2017), pp. 36–43. ISSN: 24726311. DOI: 10.1177/2211068216646741.

[8] Tae Young Kim, Dong Yeol Han, and Won Gu Lee. "Characterization of micro-circular wounds pressurized by a hybrid chip-on-dish method for live cell adhesion and mobility testing". In: *Analytical Methods* 11.9 (Mar. 2019), pp. 1174–1179. ISSN: 17599679. DOI: 10.1039/c8ay02711k.

[9] William J Ashby and Andries Zijlstra. "Established and novel methods of interrogating two-dimensional cell migration". In: *Integr. Biol.* 4.11 (2012), pp. 1338–1350. DOI: 10.1039/C2IB20154B.

[10] Ana Victoria Ponce Bobadilla et al. "In vitro cell migration quantification method for scratch assays". In: *Journal of The Royal Society Interface* 16.151 (2019), p. 20180709. DOI: 10.1098/rsif.2018.0709.

[11] Hui-Hsien Lin et al. "Chapter Six - Chemical modulation of circadian rhythms and assessment of cellular behavior via indirubin and derivatives". In: *Chemical Tools for Imaging, Manipulating, and Tracking Biological Systems: Diverse Methods for Optical Imaging and Conjugation*. Ed. by David M Chenoweth.

Vol. 639. Methods in Enzymology. Academic Press, 2020, pp. 115–140. DOI: 10.1016/bs.mie.2020.04.011.

[12] Wang Jin et al. "The role of initial geometry in experimental models of wound closing". In: (2017). DOI: 10.48550/arXiv.1711.07162.

[13] Andrea Ravasio et al. "Gap geometry dictates epithelial closure efficiency". In: *Nature Communications* 6 (July 2015). ISSN: 20411723. DOI: 10.1038/ncomms8683.

[14] Min Bao et al. "Microfabricated Gaps Reveal the Effect of Geometrical Control in Wound Healing". In: *Advanced Healthcare Materials* 10.4 (Feb. 2021). ISSN: 21922659. DOI: 10.1002/adhm.202000630.

[15] Ibidi GMBH. *Creating the Gap: Different Approaches*. URL: https://ibidi.com/content/282-creating-the-gap.

[16] Asma Nusrat, Charlene Delp, and James L Madara. *Intestinal Epithelial Restitution Characterization of a Cell Culture Model and Mapping of Cytoskeletal Elements in Migrating Cells*. Tech. rep. DOI: 10.1172/JCI115741.

[17] Masahiro Iizuka and Shiho Konno. *Wound healing of intestinal epithelial cells*. 2011. DOI: 10.3748/wjg.v17.i17.2161.

[18] Tomaz Velnar and Lidija Gradisnik. *Tissue Augmentation in Wound Healing: the Role of Endothelial and Epithelial Cells*. Dec. 2018. DOI: 10.5455/medarh.2018.72.444-448.

[19] H S Dua, J A P Gomes, and A Singh. *Corneal epithelial wound healing*. Tech. rep. 1994, pp. 401–408. DOI: 10.1136/bjo.78.5.401.

[20] Jesse R Holt et al. "Spatiotemporal dynamics of PIEZO1 localization controls keratinocyte migration during wound healing". In: *eLife* 10 (Sept. 2021). Ed. by David D Ginty and Kenton J Swartz, e65415. ISSN: 2050-084X. DOI: 10.7554/eLife.65415.

[21] Sabine Werner, Thomas Krieg, and Hans Smola. "Keratinocyte–Fibroblast Interactions in Wound Healing". In: *Journal of Investigative Dermatology* 127.5 (2007), pp. 998–1008. ISSN: 0022-202X. DOI: 10.1038/sj.jid.5700786.

[22] Hanneke N. Monsuur et al. "Methods to study differences in cell mobility during skin wound healing in vitro". In: *Journal of Biomechanics* 49.8 (May 2016), pp. 1381–1387. ISSN: 18732380. DOI: 10.1016/j.jbiomech.2016.01.040.

[23] Linlin Su et al. "Loss of CAR promotes migration and proliferation of HaCaT cells, and accelerates wound healing in rats via Src-p38 MAPK pathway". In: *Scientific Reports* 6 (Jan. 2016). ISSN: 20452322. DOI: 10.1038/srep19735.

[24] A L Rusanov et al. "Protein dataset of immortalized keratinocyte HaCaT cells and normal human keratinocytes". In: *Data in Brief* 35 (2021), p. 106871. ISSN: 2352-3409. DOI: 10.1016/j.dib.2021.106871.

[25] E. Ranzato et al. "Platelet lysate stimulates wound repair of HaCaT keratinocytes". In: *British Journal of Dermatology* 159.3 (Sept. 2008), pp. 537–545. ISSN: 00070963. DOI: 10.1111/j.1365-2133.2008.08699.x.

[26] Di Wang et al. "Vitamin D3 analogue facilitates epithelial wound healing through promoting epithelial-mesenchymal transition via the Hippo pathway". In: *Journal of Dermatological Science* 100.2 (Nov. 2020), pp. 120–128. ISSN: 1873569X. DOI: 10.1016/j.jdermsci.2020.08.015.

[27] D Gutowska-Owsiak et al. “Histamine enhances keratinocyte-mediated resolution of inflammation by promoting wound healing and response to infection”. In: *Clinical and Experimental Dermatology* 39.2 (2014), pp. 187–195. DOI: 10.1111/ced.12256.

[28] Kaitlyn R Ammann et al. “Migration versus proliferation as contributor to in vitro wound healing of vascular endothelial and smooth muscle cells”. In: *Experimental Cell Research* 376.1 (2019), pp. 58–66. ISSN: 0014-4827. DOI: 10.1016/j.yexcr.2019.01.011.

[29] Michelle Vang Mouritzen and Håvard Jenssen. “Optimized scratch assay for in vitro testing of cell migration with an automated optical camera”. In: *Journal of Visualized Experiments* 2018.138 (Aug. 2018). ISSN: 1940087X. DOI: 10.3791/57691.

[30] Simone Codeluppi et al. “Influence of rat substrain and growth conditions on the characteristics of primary cultures of adult rat spinal cord astrocytes”. In: *Journal of Neuroscience Methods* 197.1 (Apr. 2011), pp. 118–127. ISSN: 01650270. DOI: 10.1016/j.jneumeth.2011.02.011.

[31] Sergej Pirkmajer and Alexander V Chibalin. “Serum starvation: caveat emptor”. In: *J Physiol Cell Physiol* 301 (2011), pp. 272–279. DOI: 10.1152/ajpcell.00091.2011.-Serum.

[32] Yaling Huang and Lei Li. *DNA crosslinking damage and cancer - a tale of friend and foe*. June 2013. DOI: 10.3978/j.issn.2218-676X.2013.03.01.

[33] Andrew J. Deans and Stephen C. West. *DNA interstrand crosslink repair and cancer*. July 2011. DOI: 10.1038/nrc3088.

[34] Wang Jin et al. “The role of initial geometry in experimental models of wound closing”. In: *Chemical Engineering Science* 179 (2018), pp. 221–226. ISSN: 0009-2509. DOI: 10.1016/j.ces.2018.01.004.

[35] Thiruselvi Thanikachalam et al. “Gap closure of different shape wounds: In vitro and in vivo experimental models in the presence of engineered protein adhesive hydrogel”. In: *Journal of Tissue Engineering and Regenerative Medicine* 13.2 (Feb. 2019), pp. 174–178. ISSN: 19327005. DOI: 10.1002/term.2779.

[36] Amelia Ahmad Khalili and Mohd Ridzuan Ahmad. “A Review of Cell Adhesion Studies for Biomedical and Biological Applications”. In: *International Journal of Molecular Sciences* 16.8 (Aug. 2015), p. 18149. ISSN: 14220067. DOI: 10.3390/IJMS160818149.

[37] Kaivalya A. Deo et al. “Bioprinting 101: Design, Fabrication, and Evaluation of Cell-Laden 3D Bioprinted Scaffolds”. In: *Tissue Engineering. Part A* 26.5-6 (Mar. 2020), p. 318. ISSN: 1937335X. DOI: 10.1089/TEN.TEA.2019.0298.

[38] John D Lambris. *Advances in Experimental Medicine and Biology*. URL: http://www.springer.com/series/5584.

[39] Fatemeh Kabirian and Masoud Mozafari. *Decellularized ECM-derived bioinks: Prospects for the future*. Jan. 2020. DOI: 10.1016/j.ymeth.2019.04.019.

[40] Antoniac Iulian, Sinescu Cosmin, and Antoniac Aurora. “Adhesion aspects in biomaterials and medical devices”. In: 30.16 (Aug. 2016), pp. 1711–1715. ISSN: 15685616. DOI: 10.1080/01694243.2016.1170959.

[41] Piotr Stanisław Zieliński et al. "3D printing of bio-instructive materials: Toward directing the cell". In: *Bioactive Materials* 19 (Jan. 2023), pp. 292–327. ISSN: 2452-199X. DOI: 10.1016/J.BIOACTMAT.2022.04.008.

[42] Hongxu Lu et al. "Effects of poly(L-lysine), poly(acrylic acid) and poly(ethylene glycol) on the adhesion, proliferation and chondrogenic differentiation of human mesenchymal stem cells". In: *Journal of Biomaterials Science, Polymer Edition* 20.5-6 (Mar. 2009), pp. 577–589. ISSN: 15685624. DOI: 10.1163/156856209X426402.

[43] Häkkinen L, Larjava H, and Koivisto L. *Keratinocyte Interactions with Fibronectin during Wound Healing*. Austin (TX).

[44] Erkki Ruoslahti. "Fibronectin in cell adhesion and invasion". In: *Cancer and Metastasis Reviews* 3.1 (1984), pp. 43–51. ISSN: 1573-7233. DOI: 10.1007/BF00047692.

[45] Frederick Grinnell. *Fibronectin and wound healing*. 1984. DOI: 10.1002/jcb.240260206.

[46] Teruo Nishida et al. *Fibronectin Promotes Epithelial Migration of Cultured Rabbit Cornea In Situ*. Tech. rep. DOI: 10.1083/jcb.97.5.1653.

[47] Frederick Grinnell, Ken-ichi Toda, and Akira Takashima. *ACTIVATION OF KERATINOCYTE FIBRONECTIN RECEPTOR FUNCTION DURING CUTANEOUS WOUND HEALING*. Tech. rep. Dallas, TX 75235, USA: Department of Cell Biology and Anatomy, University of Texas Health Science Center, 1987. DOI: 10.1242/jcs.1987.Supplement{_}8.11.

[48] Gavin D.M. Jeffries et al. "3D micro-organisation printing of mammalian cells to generate biological tissues". In: *Scientific Reports* 10.1 (Dec. 2020). ISSN: 20452322. DOI: 10.1038/s41598-020-74191-w.

[49] *BIOPIXLAR TRANSFER MEMBRANE BIOPRINTING*. URL: https://fluicell.com/biopixlar-membrane-bioprinting/.

[50] *BIOPIXLAR® 3D SINGLE-CELL BIOPRINTING*. URL: https://fluicell.com/products-fluicell/biopixlarplatform/.

[51] Alar Ainla et al. "A multifunctional pipette". In: *Lab Chip* 12.7 (2012), pp. 1255–1261. DOI: 10.1039/C2LC20906C.

[52] Philip Wexler, ed. *Encyclopedia of Toxicology, Four Volume Set*. 3rd ed. Academic Press, Mar. 2014. ISBN: 978-0-12-386455-0.

[53] Celine Hoffmann et al. "Fluorescein isothiocyanate-labeled human plasma fibronectin in extracellular matrix remodeling". In: *Analytical Biochemistry* 372.1 (2008), pp. 62–71. ISSN: 0003-2697. DOI: 10.1016/j.ab.2007.07.027.

[54] Lalith K. Chaganti, Navneet Venkatakrishnan, and Kakoli Bose. "An efficient method for FITC labelling of proteins using tandem affinity purification". In: *Bioscience Reports* 38.6 (Dec. 2018). ISSN: 15734935. DOI: 10.1042/BSR20181764.

[55] Julia C. Arciero et al. "Using a continuum model to predict closure time of gaps in intestinal epithelial cell layers". In: *Wound Repair and Regeneration* 21.2 (Mar. 2013), pp. 256–265. ISSN: 10671927. DOI: 10.1111/j.1524-475X.2012.00865.x.

[56] Peter Friedl and Darren Gilmour. "Collective cell migration in morphogenesis, regeneration and cancer". In: *Nature reviews. Molecular cell biology* 10.7 (July 2009), pp. 445–457. ISSN: 1471-0072. DOI: 10.1038/nrm2720.

[57] Christopher Michael Gabbott and Tao Sun. "Comparison of human dermal fibroblasts and hacat cells cultured in medium with or without serum via a generic tissue engineering research platform". In: *International Journal of Molecular Sciences* 19.2 (Feb. 2018). DOI: 10.3390/ijms19020388.

[58] Bobin Mi et al. "Icariin promotes wound healing by enhancing the migration and proliferation of keratinocytes via the AKT and ERK signaling pathway". In: *International Journal of Molecular Medicine* 42.2 (2018), pp. 831–838. ISSN: 1791244X. DOI: 10.3892/ijmm.2018.3676.

[59] Marta Carretero et al. "In vitro and in vivo wound healing-promoting activities of human cathelicidin LL-37". In: *Journal of Investigative Dermatology* 128.1 (2008), pp. 223–236. ISSN: 15231747. DOI: 10.1038/sj.jid.5701043.

[60] Marc P.M. Soutar et al. *FBS/BSA media concentration determines CCCP's ability to depolarize mitochondria and activate PINK1-PRKN mitophagy*. Nov. 2019. DOI: 10.1080/15548627.2019.1603549.

[61] Gamaliel Junren Ma et al. "Quantitative assessment of bovine serum albumin proteins for blocking applications". In: (). DOI: 10.1101/869677.

[62] Daniel Fologea et al. "Electrical characterization of protein molecules by a solid-state nanopore". In: *Applied Physics Letters* 91.5 (2007). ISSN: 00036951. DOI: 10.1063/1.2767206.

[63] Linliang Yin et al. "How does fluorescent labeling affect the binding kinetics of proteins with intact cells?" In: *Biosensors and Bioelectronics* 66 (Apr. 2015), pp. 412–416. ISSN: 18734235. DOI: 10.1016/j.bios.2014.11.036.

A

Gap closure of small gaps monitored under conditions of no cell proliferation

In this appendix, representative images of gap closure of a small square gap monitored under conditions of no proliferation (condition 1) is shown. As shown in 3.3.1 Small gaps, no gap closure was not shown for gaps under this condition, which Figure A.1 aim to explain. In the figure (a) a square gap is clearly shown, however in both (b) and (c) the geometry of the gap is not intact and the initial gap has become larger.

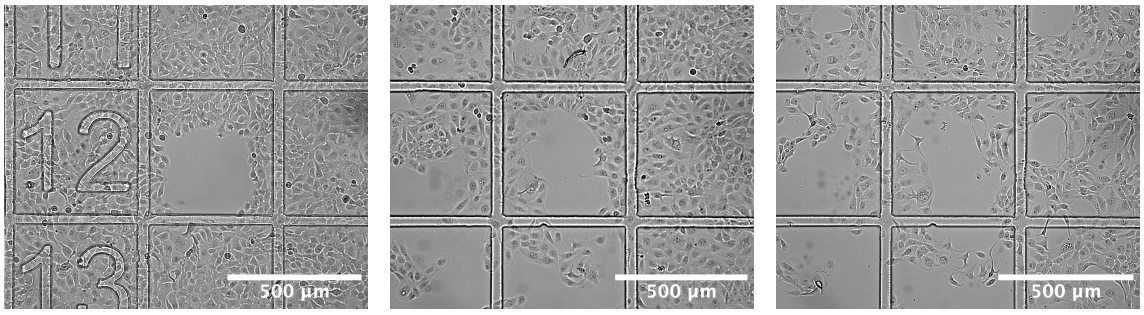

(a) **(b)** **(c)**

Figure A.1: 5X bright-field microscopy images representing closure of a small square gap monitored under conditions of no proliferation (condition 1) after (a) 0-1 hours, (b) 4 hours, and (c) 22 hours. Scale bar = 500 μm.